Journal of Applied Fluid Mechanics, Vol. 16, No. 8, pp. 1675-1689, 2023.
Available online at www.jafmonline.net, ISSN 1735-3572, EISSN 1735-3645.
https://doi.org/10.47176/jafm.16.08.1605

Effective Inverse Method for High-loaded Axial Compressor Based on Pre-compression Theory

H. Lou, H. Wu†, Q. Tang and L. Deng

School of Power and Energy, Northwestern Polytechnical University, Xi'an, Shanxi, 710129, China

†*Corresponding Author Email: wuhu@nwpu.edu.cn*

ABSTRACT

The S1 stream surface inverse method for a single-stage axial transonic compressor was developed and studied under the guidance of the quasi-three-dimensional viscous design theory, based on computational fluid dynamics (CFD), in order to establish and solve governing equations. The re--adjusted load distribution of the S1 stream surface was imposed to obtain a special profile for the rotor, which is known as S-shaping. This changed the structure and weaken the strength of the shock due to the pre-compression effect. In order to match the inlet flow angle of the downstream stator, inverse modification for multiple S1 stream surfaces of the stator blade was conducted in the present study at the same time. As it is known, the S-shaped profile is commonly applied to supersonic flows. Therefore, NASA stage 37 was selected as the design case to verify whether the present inverse method is effective and reliable. Stage 37 was re-designed by stacking five S1 stream surfaces. The profiles of these surfaces were renewed through the inverse design. The results revealed that, compared to the prototype, the aerodynamic performance of the re-designed one was apparently promoted within the stable working range. The adiabatic efficiency at the design point increased by approximately 0.4%, and the pressure ratio improved by approximately 4.5%. In addition, analysis result for the characteristic line revealed that the performance of the redesigned blades at off-design points significantly improved.

Article History

Received October 12, 2022
Revised March 19, 2023
Accepted April 6, 2023
Available online May 31, 2023

Keywords:

Axial transonic compressor
Aerodynamic performance
Inverse method
Shock wave
Pre-compression

1. INTRODUCTION

The merits and demerits of compressor aerodynamic performance critically influences the stable work of an aircraft engine. The booming development of the aviation industry requests for the aircraft engine to have a more excellent performance, in order for the compressor which is considered the core component of an engine, to have a better component performance as well. As a result, the development trend of compressor design methods was to make compressor have a higher total pressure ratio and efficiency, and make the compressor work at a wider stability margin.

Professor Wu Zhonghua proposed the two-kinds-of-stream-surface theory, and a quasi-three-dimensional compressor blade design system was developed based on this research in 1952 (Wu, 1952). The traditional compressor design method was employed to finish the initial blade geometry design and flow analysis through the one-dimensional average radius design, the two-dimensional axisymmetric throughflow design and three-dimensional performance analysis and optimization. It is essential to constantly justify the blade geometry and repeatedly solve the flowing structure, when the flow structure does not satisfy the blade design aerodynamic performance, until the design requirement is reached. CFD technology plays an important role in the present axial compressor flow analysis system, and this was applied to calculate the detail flow filed at the design procedure. This is a well-known analytical method. However, the abovementioned repeating trial and error progress consume a lot of time, causing the design cycle to be longer, and the design efficiency to be pretty low.

The inverse method is a typical design method that deals with the situation of having a complicated procedure in an analytical method. By conducting numerical simulations on the initial geometry based on the CFD technique, the flow filed distribution can be obtained. The designers can modify the aerodynamic parameter (isentropic Mach number, pressure, load, velocity, etc.) distributions, in terms of the targeted aerodynamic performance. The modified aerodynamic parameter distribution is substituted into the inverse method solver

Nomenclature

CFD	Computational fluid dynamics	$\Delta t, \Delta t_{flow}$	Time step of the inverse method and local time-stepping
RANS	Reynold-averaged Navier-Stokes equations	$v_n^{\pm}$	Normal updating velocity of the blade suction and pressure surface
JST	Jameson Schmidt Turkel	γ	Specific heat ratio
LU-SGS	Lower-Upper Symmetric Gauss-Seidel	$p^{\pm}$	Static pressure of blade suction and pressure surface
U	Conservative variables	$(\ )^{new}$	Variables after the redesign
F, G	Convective flux	$p_{avg}, \Delta p$	Average pressure and the load
F_v, G_v	Viscous flux	Δf	Virtual displacement
S	Source term	c	Chord of the cascade
$n_{ij}^{\pm}$	Normal unit vector of blade profile		

as a design target. As a result, a new blade geometry that satisfies the design attention can be straightly obtained by taking control of the aerodynamic parameter distribution on the blade surface. In conclusion, the inverse method directly links the aerodynamic parameter distribution with aerodynamic performance, allowing the overall design procedure to be further simplified, and more purposeful.

At the beginning, the inverse method was mainly applied to the design of the two-dimensional blade cascade. Lighthill posed the concept of the airfoil inverse method. The theory obtained the analytic solution for the incompressible two-dimensional flow, based on the potential flow equation. Then, the airfoil was calculated using the prescriptive velocity field (Lighthill, 1945). In the 1980s, the inverse design idea on turbomachinery was put forward by Hawthorne. This was conducted in the situation of prescriptive average tangential velocity distribution under the assumption of inviscidity and incompressibility (Hawthorne et al., 1984; Tan et al., 1984).

As CFD technology becomes increasingly developed, the inverse method has been gradually utilized in engineering practice. The detailed research on the inverse method was implemented under Dang's group, from the two-dimensional inviscid design calculation, to the three-dimensional viscous calculation, and the research object extends from the subsonic compressor to the transonic compressor (Dang, 1993, 1995; Medd et al., 2003). The permeable boundary condition, which is applicable for the inverse design calculation, was improved, and an inverse design program for the axial compressor called, INV3D, was exploited. The inverse design theory of Zangeneh was similar to that of Dang, while the difference was that the former successfully applied Dang's method to the viscous flow (Zangeneh et al., 1998, 1999; Tiow & Zangeneh 2000). Ghaly made a solution for the virtual velocity of the camber line through the differences between the subscribed load and initial load, and the blade geometry can be renewed based on this virtual velocity (Ahmadi & Ghaly, 1998). The aerodynamic matching progress of the compressor stages was simplified by researching the inverse method of multi-stages, and the engineering practicability of the method was promoted by Hield and Van Rooij (Hield, 2008; van Rooij & Medd, 2012). Yang researched the details of the existence and uniqueness of the inverse design method, raised a method to solve the non-unique problem, developed the permeable boundary conditions, and constructed an inverse design method system by solving the full three-dimensional Navier-Stokes equations, based on the finite volume method (Yang et al., 2015, 2016). Liu established a loading-camber and static pressure-profile inverse design system, developed a series of more practical adminicular software, and carried out modification designs for a variety of axial compressors, achieving a good result (Liu, 2017; Liu et al., 2015).

Modern CFD technology exhibits accuracy in the prediction of the sophisticated viscous flow. The present inverse method already has a stable solution procedure, and the calculated results fit the prescribed aerodynamic parameter distribution well with constant development. This shows that the inverse method takes a certain status in the turbomachine design filed. In the present study, the improved inverse method of the S1 stream surface was presented. Success was achieved due to the pre-compression effect, which combines the theory of the quasi-three-dimensional viscous flow, and the superiority of the inverse method. It is noteworthy that the quasi-three-dimensional solver demonstrates great calculation efficiency. When compared to fully three-dimensional cases. To the author's best knowledge, the new inverse method for the pre-compression blade, based on the S1 steam surface of the single-stage high-load axial transonic compressor, has not been implemented in open literature.

The remainder of the article is organized, as follows. Section 2 presents the theoretical governing equations, specific numerical method, and detailed inverse method implemented. In sections 3 and 4, the effectiveness was validated in two application cases, which comprised of the high-loading Rotor 37 and Stator 37. Finally, the meaningful and innovative conclusions were summarized in section 5.

2. MODEL AND CALCULATION METHOD

Figure 1 presents the transformation between the S1 stream surface coordinate system and cylindrical coordinate system. By applying the basic assumption of the revolution surface to the RANS equations in the relative cylindrical coordinate system, the governing equations of any revolution surface (the S1 stream surface) in the coordinate system can be employed, as

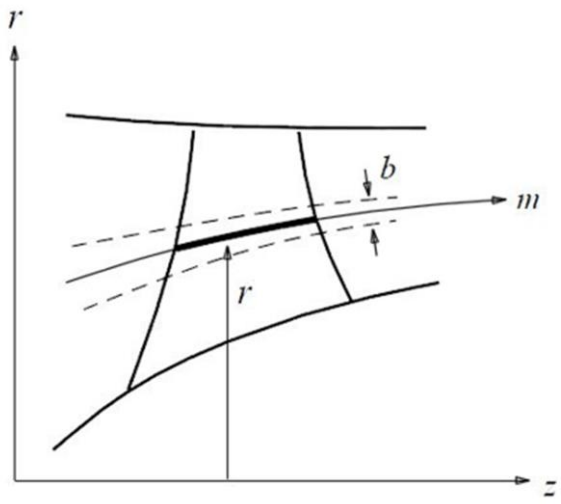

Fig. 1. The transformation between the S1 stream surface coordinate system and cylindrical coordinate system.

follows:

$$\frac{\partial U}{\partial t}+\frac{1}{rb}\left[\frac{\partial rb(F-F_v)}{\partial m}+\frac{\partial b(G-G_v)}{\partial \varphi}\right]=S \tag{1}$$

Where: m refers to the meridian coordinate, φ refers to the relative angular coordinate, S refers to the source term, taking into consideration the centrifugal force caused by the change in thickness (b) and radius (r) of the stream surface. The equations to be solved were the Navier-Stokes equations in the integral form, which were calculated using the finite-volume method, based on the cell-centered scheme. The second order central difference scheme was applied for the spatial discretization of the viscous flux. The JST scheme was applied for the spatial discretization of the convective flux (Jameson et al., 1981). The LU-SGS implicit scheme was adopted for the time-marching procedure. The local time-stepping method was utilized to accelerate the solving progress of the governing equations (Blazek, 2015). The internal flow in axial compressors was assumed to be fully turbulent, and the Baldwin-Lomax turbulence model was employed to simulate the turbulent viscosity, and ensure the accuracy of the solver (Baldwin, 1978). The computational domains were discretized into the structured H-type mesh. The boundary conditions in the solver include the following: non-reflective inlet, static-pressure outlet, periodic boundary, no-slip wall, and the non-reflective mixing plane model (adopted in the stage case). On this basis, a program to analyze the quasi-three-dimensional flow of axial compressors was developed. It should be noted that the effect of the blade thickness and blade radius on the flow was fully considered in the procedure, making the flow environment closer to the three-dimensional characteristics of compressor flow.

2.1 Inverse Method Theory

The design course of the axial compressor is actually a procedure of continuous iteration and repeated repetition of the analytical and inverse calculations. The analytical calculation was the step to solve the aerodynamic performance of the compressor, on the basis of the known blade geometry. In the contrary, the inverse calculation was the procedure to solve the geometry of the blades through the prescriptive aerodynamic parameters of the flow field.

Based on the theory of the S1 stream surface viscous flow solver and the inverse method theory, the present study developed a quasi-three-dimensional inverse method that varied from the full three-dimensional method, taking the different sections of the blade as the design object of the inverse calculation. Compared to the full three-dimensional viscous inverse design, the quasi-three-dimensional inverse design have unique advantages.

The previous analysis revealed that in the inverse design, the aerodynamic parameters of the compressor blades were the design variables, while the geometric configuration of the compressor blades was the design target. Usually, the designer will provide the blade aerodynamic parameter distribution, according to the design requirements. There are many approaches to regulate these aerodynamic parameters. The blade surface pressure loading can be specified, that is, the static pressure difference between the blade suction and pressure surface, or the static pressure distribution of the blade suction and pressure surface, the velocity distribution, and so on. Based on relevant domestic research, the present study combined the advantages of two inverse design methods, and created a new and improved design method.

The so-called loading-camber method: Taking the blade surface pressure load distribution as the design variable and the blade mid-curved surface as the design goal, the thickness of the blade remained unchanged during the design calculation procedure, and the mid-curved surface continuously changed until the specific blade surface load distribution was satisfied. The advantage of this method is that the blade load reflects the work transfer between the blades and the airflow. By adjusting the load, the amount of work added to the airflow by the compressor blades can be effectively controlled, thereby controlling the total pressure ratio of the rotor blade outlet, the airflow angle of the stator blade outlet, and other parameters.

As shown in the previous research, the implementation procedure of the loading-camber inverse method had no direct relationship with the actual aerodynamic parameters. Taking this into account, a new pressure-profile method was established by Liu. The construction of the inverse method and design of the boundary condition was based on the following two principles: first, the no-slip wall boundary was used as the basis to better meet the viscosity calculation requirements; second, the conservation of the flow characteristic variables at the wall was constant before and after the blade profile was updated. The relationship between the aerodynamic parameters in the flow field and the change in blade profile was established. Based on these above principles, Liu adopted the conservation of Riemann invariants to construct a new inverse design boundary condition, which was called, the pressure-profile method.

The so-called pressure-profile method: the blade suction and pressure surface static pressure distribution

were taken as the design variables, and the blade suction and pressure surface profile were taken as the design goal. During the design calculation course, the blade suction and pressure surface profile will continue to change under the prescriptive static pressure distribution, until this is satisfied. This method is more flexible, and its main advantage is that it can achieve a more refined control of the flow field near the blade surface, and in the blade channel, achieving the design goals, such as reducing separation, and changing the intensity and position of the shock wave.

In the actual implementation process, the pressure-profile method had certain disadvantages. For example, since its essence is to directly modify the geometry of the blade surface, the pressure adjustment margin of this method was narrow. Otherwise, the calculation would be difficult to converge.

Considering the limitations of the above two methods, the present study developed an improved inverse method.

The inverse theory of Yang, J. and Yang, C. provides guidance for the present study. Yang, C. calculated the normal updating velocity of the blade suction and pressure surface (Yang et al., 2017, 2019):

$$\left(v_n^{\pm}\right)^{new} = \frac{2}{\gamma - 1}\sqrt{\frac{\gamma}{\rho^{\pm}}}\left(\sqrt{\left(p^{\pm}\right)^{new}} - \sqrt{p^{\pm}}\right) * sign(\pm 1) \tag{2}$$

$$\left(p^{\pm}\right)^{new} = p_{avg} \pm \frac{1}{2}\Delta p \tag{3}$$

It can be concluded from Equation (2) that the virtual normal velocity of the wall is driven by the static pressure difference before and after the update. However, by converting the load with static pressure, the relationship between the load and virtual speed can be established. At the same time, the virtual displacement of the camber line can be presented, as follows,

$$\Delta f = \frac{1}{2}\left(\left(v_n^{+}\right)^{new} * n_\theta^{+} + \left(v_n^{-}\right)^{new} * n_\theta^{-}\right) * \Delta t \tag{4}$$

$$\Delta t = \min\left(\frac{0.01c}{\max(v_i)}, \Delta t_{flow}, 0.01\right) \tag{5}$$

Equation (4) shows that the virtual velocities of the suction and pressure surfaces were averaged to obtain the displacement of the camber line. The optimal time step was presented in Equation (5), in order to allow this to converge at the fastest rate during the inverse calculation.

2.2 Concrete Chart for the Inverse Design Method

The present study developed the inverse design method of the S1 stream surface based on the above-mentioned inverse design theory. At the beginning of the design procedure, five design S1 stream surfaces were constructed, according to the construction method for S1 stream surfaces. A detailed characteristic curve was drawn by respectively conducting the analytical numerical simulation on the five design sections. Then, the near peaking efficiency point was selected among the whole characteristic curve points, in order to carry out the inverse design. The original load distribution of each point was reasonably modified, aiming to improve the efficiency and aerodynamic performance of every S1 stream surface. Furthermore, the situation of the total load was nearly maintained constant. As a result, the whole blade was able to operate on the condition of satisfying the higher performance requirement.

It was obviously presented that the inverse design theory was built on the basis of the relationship between the load distribution differences and camber line coordinate. This allows for the modified load distribution to be given by researchers and designers, in the case of making the total load on every S1 stream surface unchanged. The modified load distribution was regarded as the design target, and was placed into the inverse design code. Afterwards, the inverse calculation was carried out. At the same time, the new S1 Stream surface geometry configuration, in which the aerodynamic performance was promoted, was shaped through the continuous updates of the stream surface camber line. Finally, the new full-span axial compressor blade was formed by stacking the S1 stream surfaces one by one, which includes five redesigned surfaces. The hub and tip profiles were the same as the original geometries, and the geometry configurations of the other sections along the radial direction were acquired through interpolation. Then, the aerodynamic performance of the new redesigned blade at the on-design and off-design point was compared with the original one by carrying out the numerical simulation validation. This is essential to verify the effectiveness and efficiency of the inverse method on the S1 stream surface. The flowchart for the inverse design method on the S1 stream surface is presented in Fig. 2.

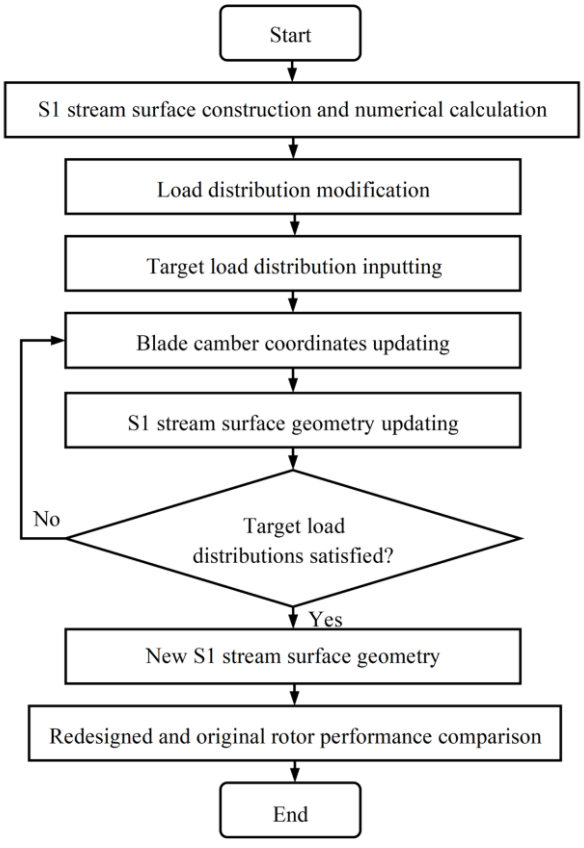

Fig. 2. Flowchart for the inverse design method on the S1 stream surface.

Compared to the fully three-dimensional viscous calculation, the inverse design method for the S1 stream surface conducts research on a certain or some stream surfaces along the spanwise, and the grid nodes on the spanwise are significantly decreased. As a consequence, the computation speed is greatly increased, causing this to take a shorter time to achieve the aerodynamic performance of the design sections. That is the reason why the method is convenient for the research of the aerodynamic performance of a certain S1 stream surface, and its influence on the overall performance of a whole blade. Furthermore, the inverse method is more purposeful and efficient.

3. REDESIGN OF THE ROTOR

In order to illustrate the capacity of the inverse method, the blade geometry was redesigned by choosing Rotor 37 and Stator 37 as the design case in the present study. Rotor 37 is a high-loaded axial compressor rotor blade, which has a very strong passage shock-wave. The boundary layer sharply thickens after the shock-wave intersects with the suction surface, due to the biggish adverse pressure gradient, eventually causing a wake flow separation. The original rotor was designed using multiple-circular camber airfoils (MCA) with 36 blades. The aspect ratio was 1.19.

The Rotor 37 test report (Suder, 1996) provides the detailed distribution of the flow field under 92.5% and 98% choking mass-flow conditions at the designed rotational speed. The present study selected the corresponding operating point for numerical simulation, and compared the flow field flow results with the test report, as shown in Figs 2 and 3.

As shown in Fig. 3, the numerical simulation and experimental flow field distribution at the 70% blade height position under 98% choking flow condition were compared.

As shown in Fig. 4, the inflow flows at a relative supersonic speed, reaching 1.4 at the wave front. A strong positive shock wave extends from the leading edge of the blade to the suction surface of the adjacent blade, and the interaction between the shock wave and boundary layer causes a flow

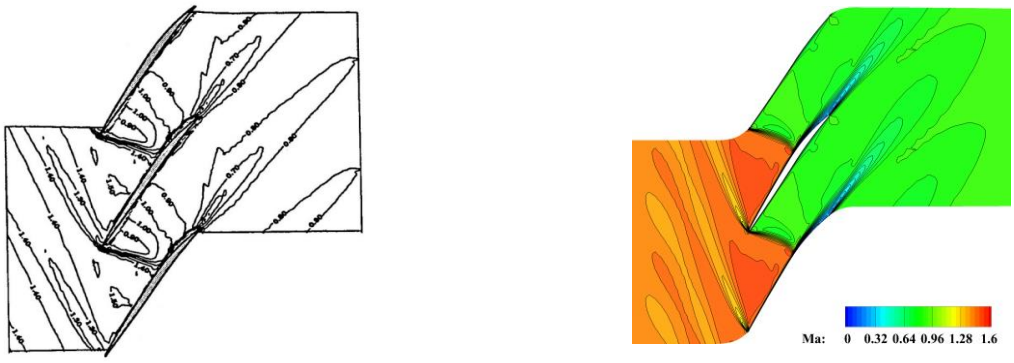

Fig. 3. Comparison of the test report and result simulated at 70% span under 98% choking mass-flow condition.

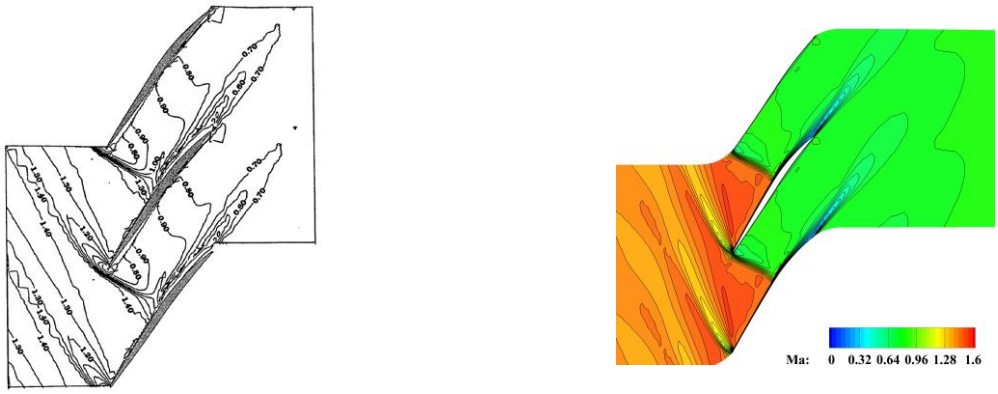

Fig. 4. Comparison of the test report and result simulated at 70% span under 92.5% choking mass-flow condition.

separation. Compared to the 92.5% choking flow condition, the positive shock wave position of the channel was more rearward, and approximately 55% of the chord length was at the intersection of the suction surface. The calculated and experimental Mach number of the wave front was 1.4. The above flow phenomena were in good agreement with the experimental results. At the same time, compared to the experimental results, the numerical simulation results were able to more accurately capture the shock wave structure and its location information, as well as the location and area of flow separation after the wave, verifying the reliability and accuracy of the numerical simulation software.

3.1 Load Distribution of Rotor 37

In order to apply for a higher inflow Mach number, a pre-compression blade profile was developed. The angle at the front section of the blade suction surface became negative. The supersonic flow through the special zone of the blade profile was not be expanded and accelerated, but this was compressed and decelerated, effectively reducing

the Mach number in the front of the shock wave (Chu et al., 2009). In engineering practice, when the inlet Mach number reaches 1.5 or higher, the precompression blade profile with a S-shape in the middle camber is usually adopted. The blade profile can effectively control the shock intensity, and reduce loss (Hu, 2014). Therefore, this section reorganizes the shock wave structure by providing a prescribed load distribution, and carrying out a pre-compression customized blade design for the supersonic S1 flow surface, thereby exploring the impact of the shock wave structure on the shock wave intensity and flow field detail distribution.

According to the pre-compression theory mentioned above, the present study reorganized the single normal shock-wave to a structure of pre-compression wave, combined with oblique-waves. As a result, the relative Mach number before the shock-wave decreased, and the shock-wave strength apparently weakened. Figures 5a-5e present the static pressure distribution and corresponding load distribution on the suction and pressure surfaces, before and after the modification of the inverse design, at the near peak efficiency points on the five S1 stream surfaces. As shown in the figure, the static pressure adjustment method was, as follows: on the suction surface, the airflow initially undergoes a short period of accelerated and depressurized flow along the leading edge, followed by a pre-compression wave, which was due to the presence of a negative angle on the suction surface of the S-shaped blade. Due to its deceleration and pressurization effect on the air flow, the static pressure would gradually increase, and the relative Mach number would gradually decrease, but will remain supersonic. Then, due to the changes in suction surface of the S-shaped blade, from a negative angle to a positive angle, the supersonic airflow expands and accelerates along the suction surface, forming a weak oblique shock wave. Finally, the airflow passes through the weak oblique shock wave to decelerate and pressurize. On the pressure surface, due to the S-shaped structure of the blade profile, the pressure surface should initially protrude into the flow channel, and subsequently concave out the flow channel. Therefore, the airflow should be initially accelerated and depressurized, and subsequently decelerated and pressurized.

3.2 Profile changes of Rotor 37

The original and inverse profile of the S1 stream surface at five different spanwise locations are presented in Fig. 6. There is very little change at the leading edge, and there is a pretty visible change at the second half of chord, as a concrete manifestation of the profile transforms to the S-shape, specifically at 70% and 85% span. The reason for the formation of this typical structure was because the blade profile changed into a concave, rather than into a convex, at approximately 20% to 50% of chord, and the second half of the chord had a more apparent convex, when compared to the original one.

The airflow was compressed, rather than expanded, along the suction surface due to the concave contour. This compressed function is called, pre-compression, which leads to the decline in Mach number in the front of the shock-wave. Thus, the strength of the shock would be impaired, and the shock loss would be reduced. On the other hand, the development trend of the boundary layer would be weakened, because the whole flow turning angle becomes smaller. This explains why the reverse pressure gradient near the trailing edge of the modified suction surface was smaller than that of the prototype. According to the viscous mechanics theory, this will reduce the loss near the trailing edge, and the thickness of the boundary layer will be reduced.

3.3 Mach Number Contour Analysis of Rotor 37

The solution refers to the comparison of Mach number contours, between the original (upper plots) and inverse (lower plots), at the different spanwise locations presented from Fig. 7 to Fig. 11. These figures show that the Mach number contour structure significantly changed. This mainly manifested due to two aspects. On one hand, the shock shape is altered to an oblique shock from an almost novel shock at the spans near to hub, such as the 15% span. Then, these turns to the combined shape for the pre-compression wave and oblique shock at the tip sections, such as the 70% span and 85% span. On the other hand, the acceleration zones of inverse profile become smaller, when compared to that of the original, while the Mach number in the front of the shock wave becomes visibly smaller.

It is well-known that the airflow velocity would decrease under the function of the shock-wave. This would cause the decelerating effect of the shock-wave in the inverse design to become significantly smaller, because the shock structure changed, and the shock strength became weaker. Consequently, the adverse pressure gradient will also become smaller. As a result, the flow loss caused by the discontinuity of the shock-wave becomes weakened, and the adiabatic efficiency becomes promoted, accordingly. As shown in Figs 7-11, the wake along the suction surface achieved an obvious reduction.

The aforementioned inverse design results corresponded with the expected effects. Thus, the design intention of improving the aerodynamic performance was achieved.

3.4 Aerodynamic Performance Analysis of the Rotor Blade

A whole new rotor blade, which was formed by stacking the above five design stream surfaces, original hub and tip sections, was simulated using the three-dimensional solver to attain the flow filed distribution.

The phenomenon presented in Figs 12-13 refers to the comparison of Mach number distributions between the original and redesigned rotor blade at the suction or pressure surface. The normal shock wave was reformed to a pre-compression wave

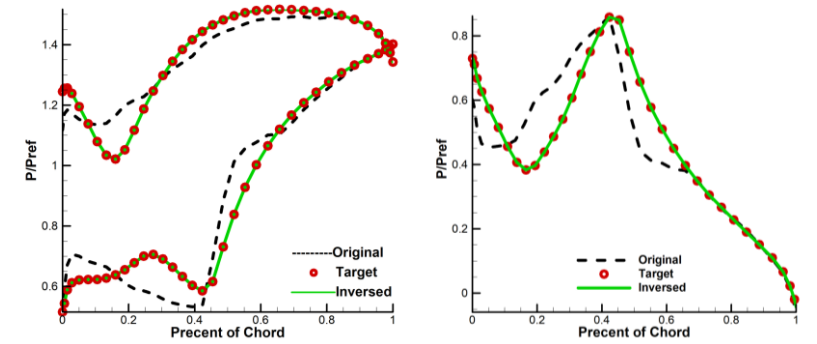

(a) Pressure and load distribution at 15% span

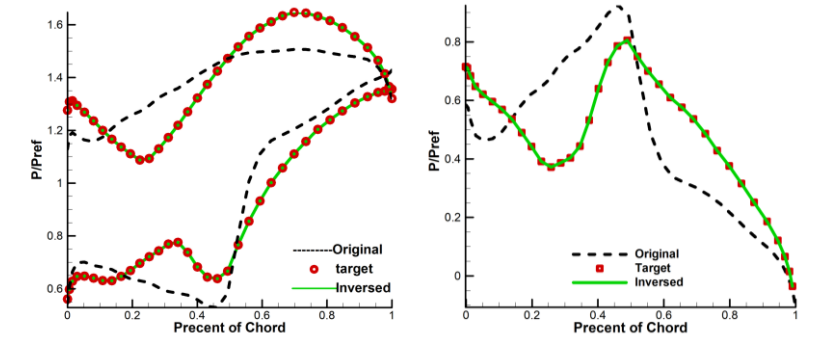

(b) Pressure and load distribution at 30% span

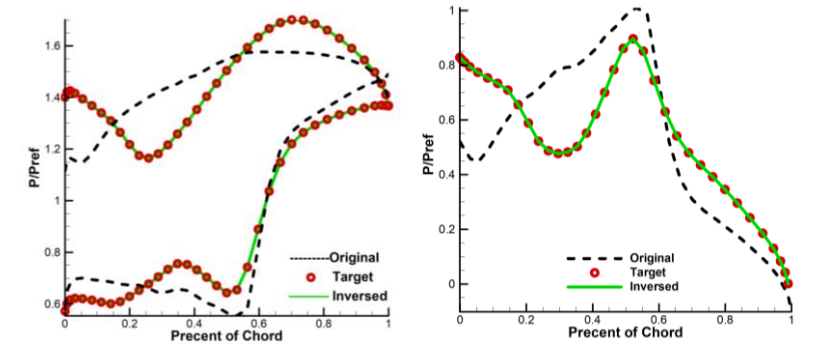

(c) Pressure and load distribution at 50% span

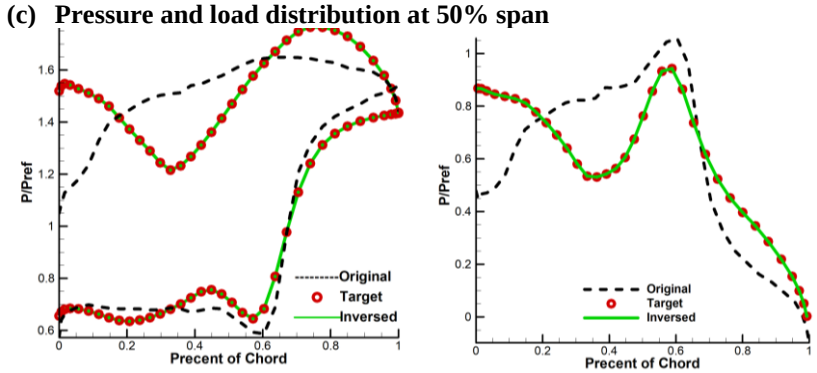

(d) Pressure and load distribution at 70% span

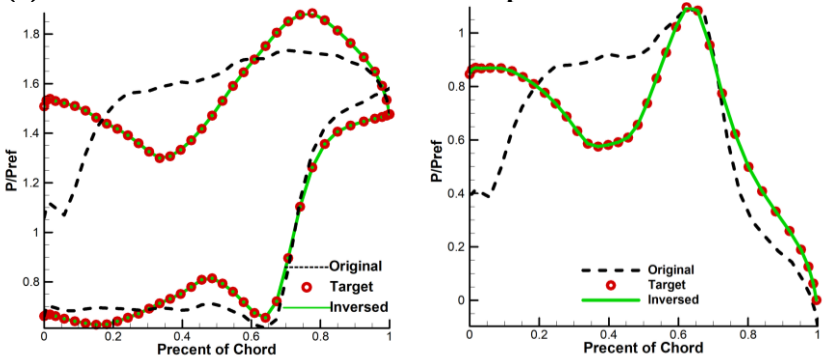

(e) Pressure and load distribution at 85% span

Fig. 5. Comparison of original and inverse pressure and load distribution at five spans.

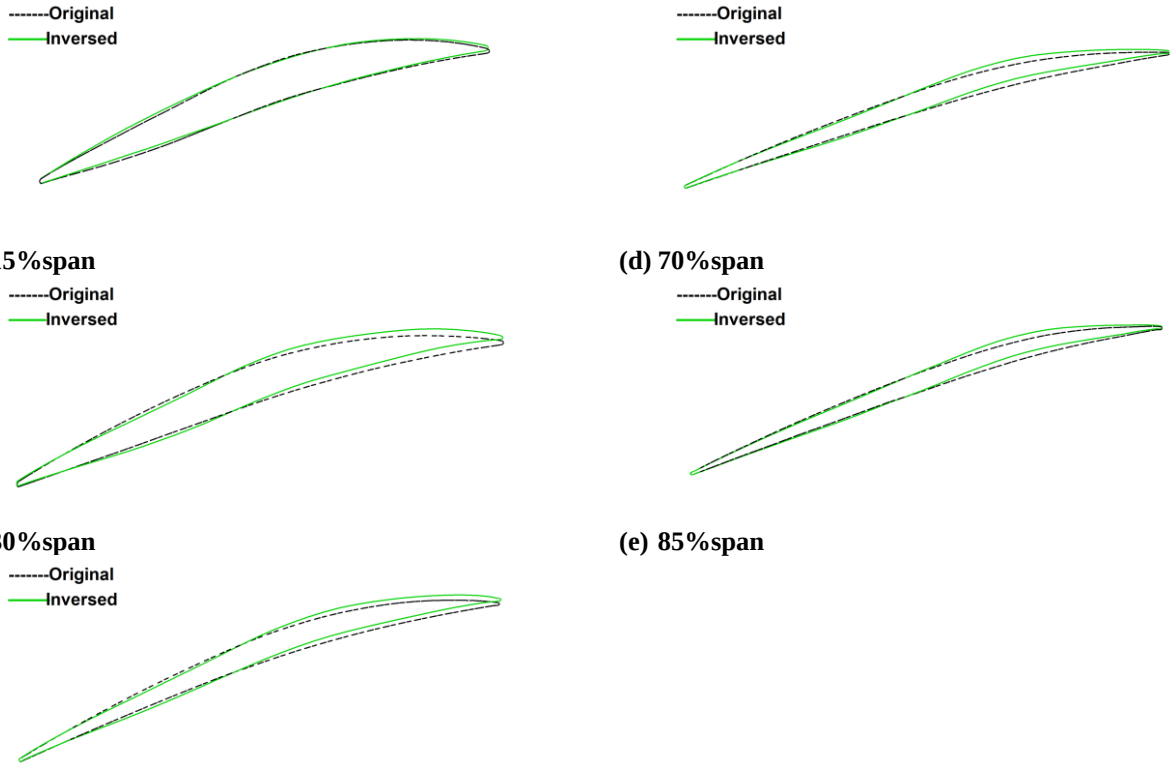

Fig. 6. Comparison of the original and inverse profile at the five spans.

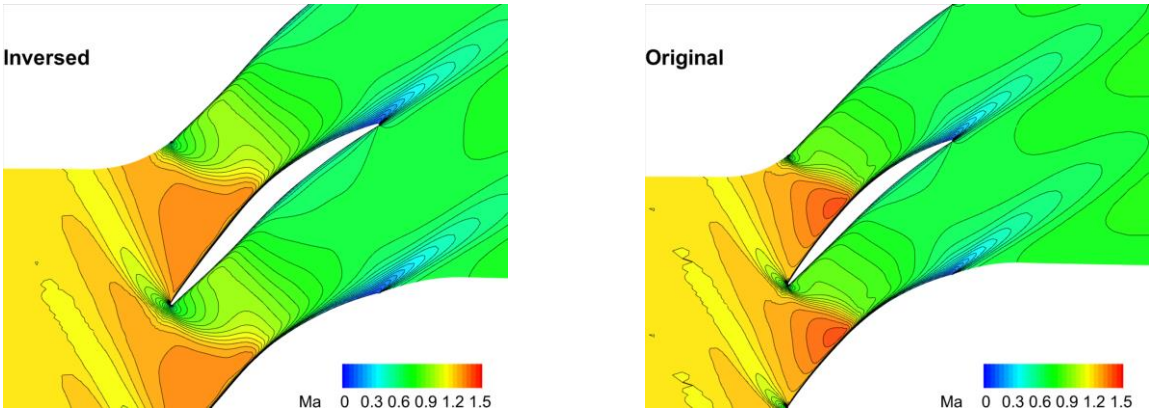

Fig. 7. Comparison of Ma contour between the original and redesigned S1 stream surface at 15% span of the blade.

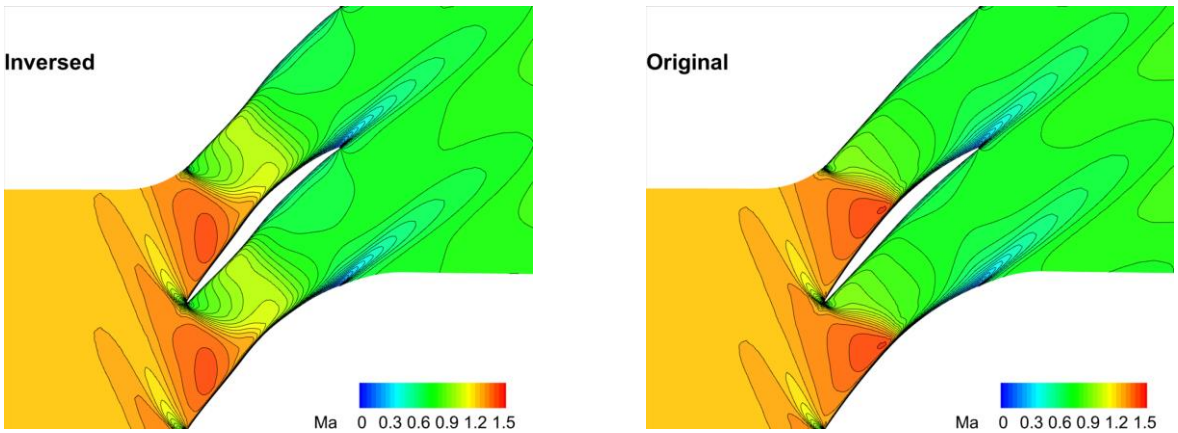

Fig. 8. Comparison of Ma contour between the original and redesigned S1 stream surface at 30% span of the blade.

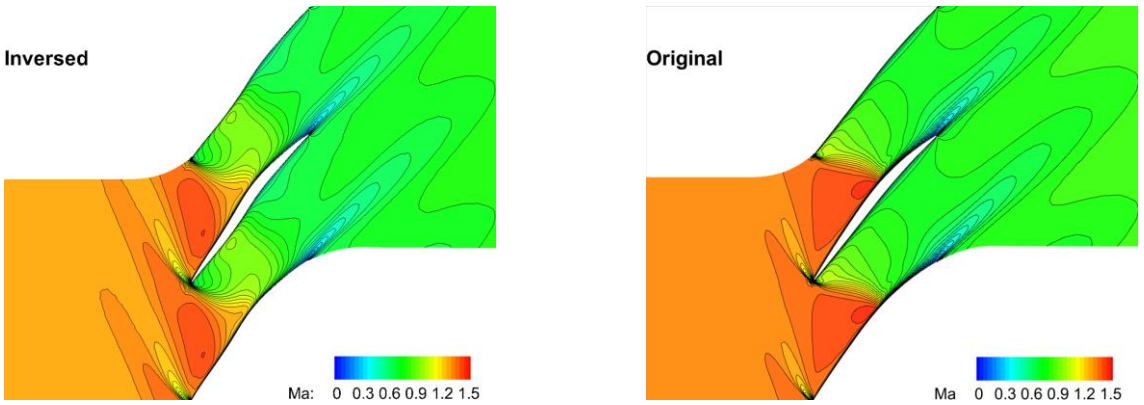

Fig. 9. Comparison of Ma contour between the original and redesigned S1 stream surface at 50% span of the blade.

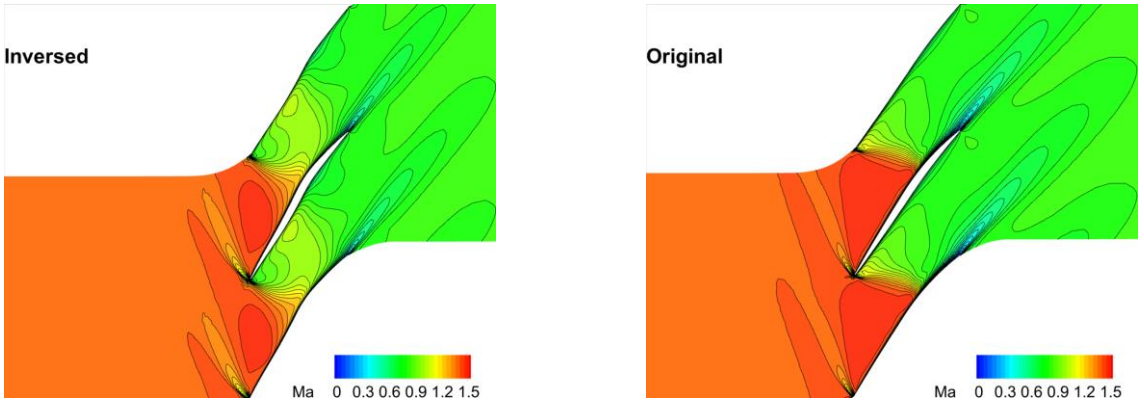

Fig. 10. Comparison of Ma contour between the original and redesigned S1 stream surface at 70% span of the blade.

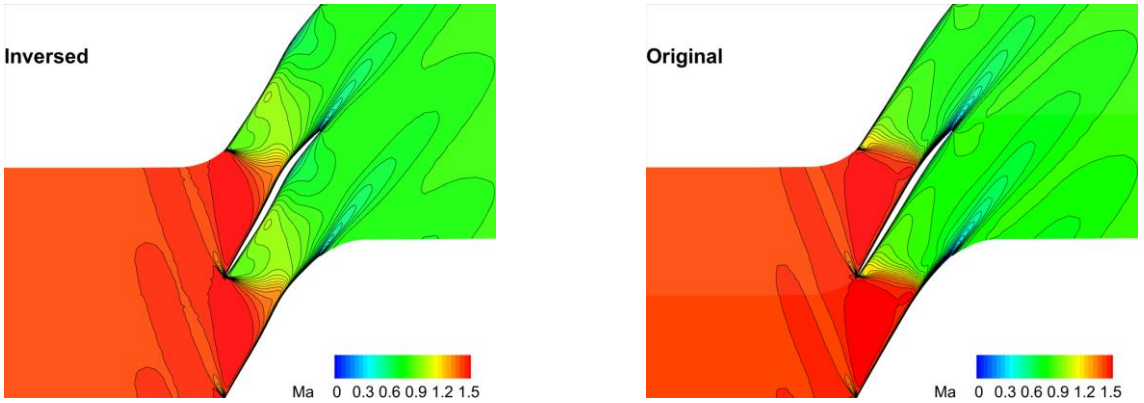

Fig. 11. Comparison of Ma contour between the original and redesigned S1 stream surface at 85% span of the blade.

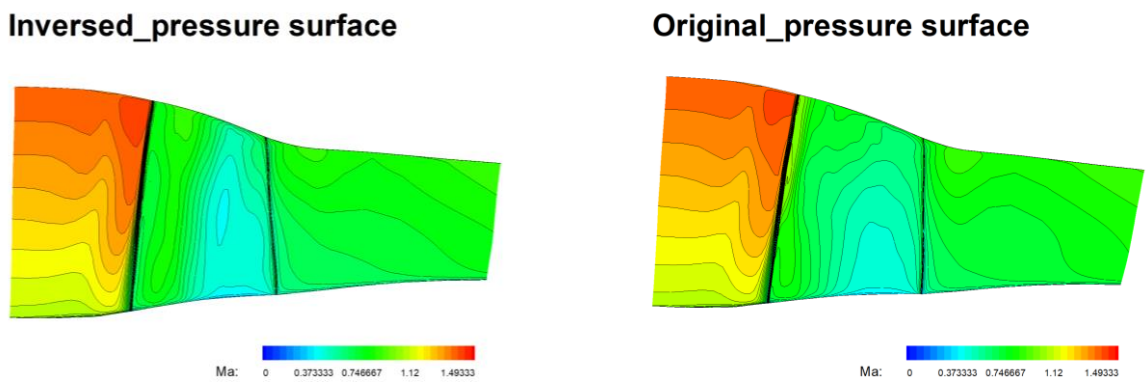

Fig. 12. Comparison of Ma contour between the original and redesigned rotor blade at the pressure surface.

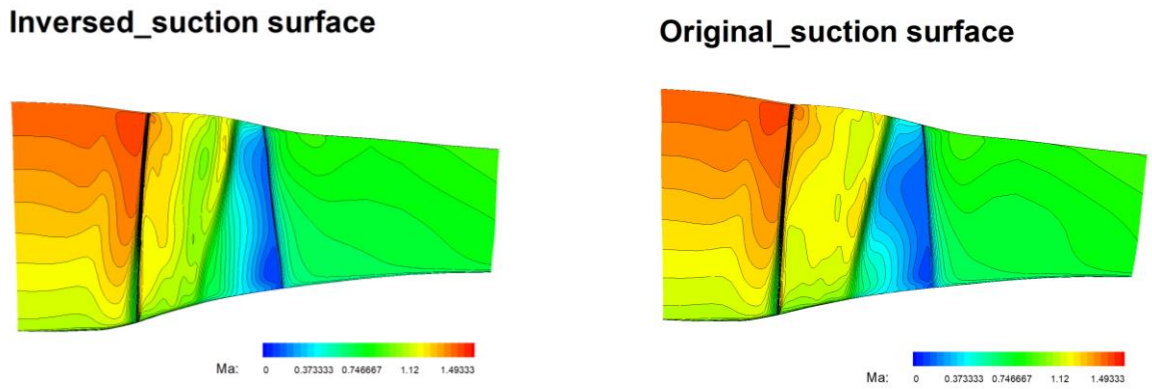

Fig. 13. Comparison of Ma contour between the original and redesigned rotor blade at the suction surface.

Table 1 Aerodynamic parameter comparison at the design point for Rotor 37

	Mass(Kg/s)	Adiabatic Efficiency	Pressure Ratio
Initial Rotor Bade	20.8372	0.883369	2.10047
Redesigned Rotor Bade	21.0283	0.896193	2.13239
Increasing percentage	0.91711%	1.2824%	3.192%

combined with a weaker oblique shock wave. As a result, the strength of the shock correspondingly became smaller. Obvious evidence revealed that the zones near the stall remarkably decreased from the suction.

Table 1 presents the comparison of aerodynamic parameters at the on-design point, between the original and redesigned rotor blade. This shows that the choking mass increased by 0.91711%, the adiabatic efficiency improved by 1.2824%, and the pressure ratio was promoted by 3.192%, respectively.

In terms of the inverse design at near peaking point, the aerodynamic performance was promoted, especially for the redesigned rotor blade. A more profound consideration is that the results can be utilized in a compressor stage to improve the aerodynamic performance. In addition, this can be employed into engineering practice.

Figures 14 and 15 presents the adiabatic efficiency and pressure ratio characteristic comparison between the original and redesigned rotor blade, respectively. It can be visually observed from the diagram that the stable working range of the redesigned rotor blade was broader, when compared to that of the original one. This shows that the choking mass flow is larger, and the surge is smaller.

The adiabatic efficiency and pressure ratio characteristic curve for the redesigned rotor blade was obviously higher, when compared to that of the original one, at the whole operating range. It was obtained by calculation that the adiabatic efficiency approximately increased by 1.28%, and the pressure ratio increased by approximately 3.19%. These results indicate that the inverse method for the S1 stream surface can well-satisfy the design target, and that the aerodynamic performance of the redesigned blade was better, when compared to that of the original one, at the whole working range, in the situation of a designed rotational speed.

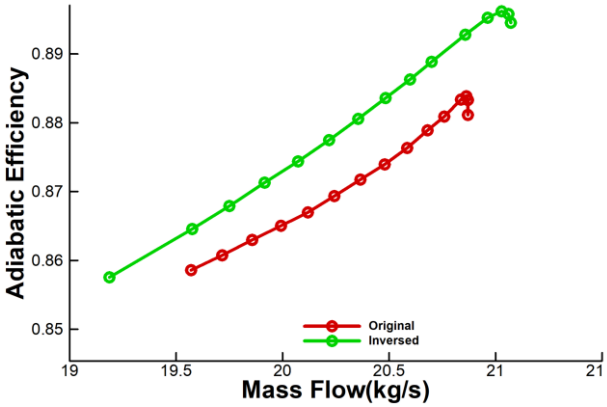

Fig. 14. Comparison of adiabatic efficiency between the original and re-designed rotor blade.

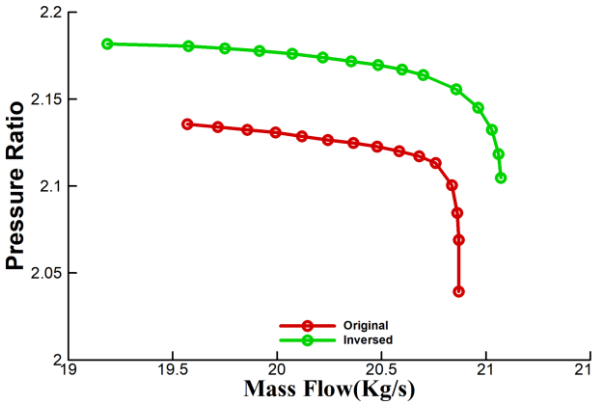

Fig. 15. Comparison of pressure ratio between the original and re-designed rotor blade.

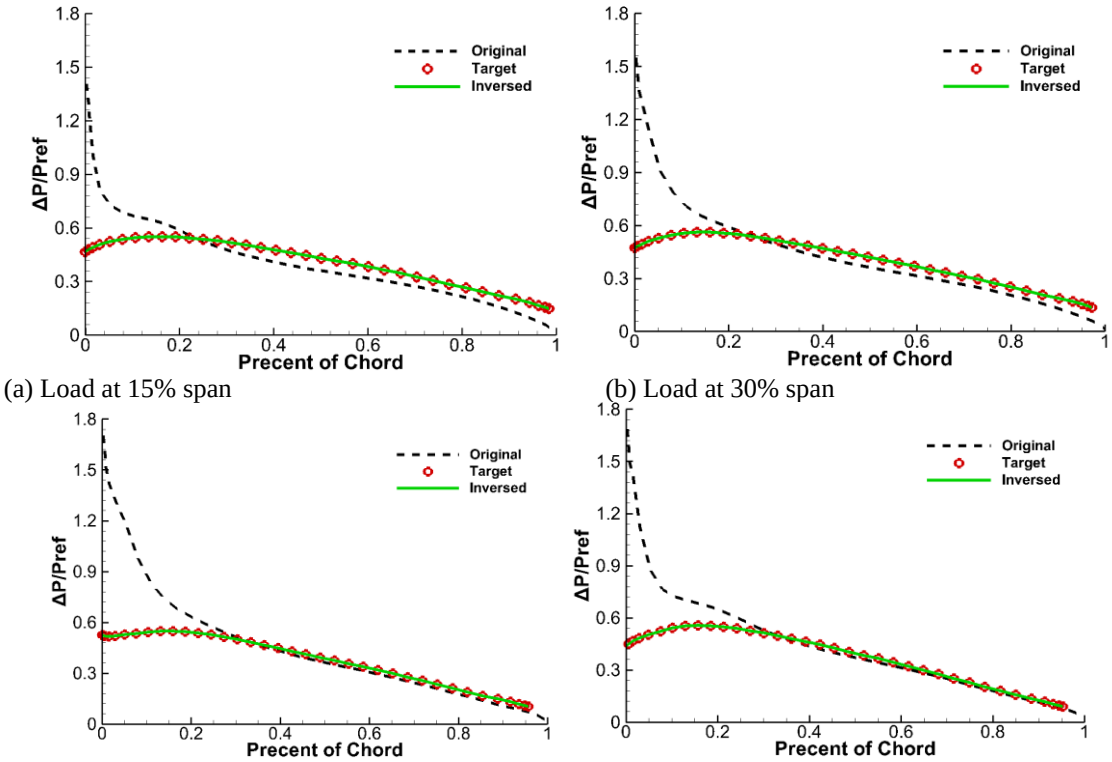

(a) Load at 15% span (b) Load at 30% span

(c) Load at 50% span (d) Load at 70% span

Fig. 16. Comparison of original and target load distribution at four spans.

4. FURTHER MODIFICATION OF A SINGLE COMPRESSOR

In the above sections, the S1 flow surface inverse modification was carried out on Rotor 37, and a new rotor blade with significantly improved aerodynamic performance was obtained. Due to the modification design, the airflow angle at the outlet of the rotor blade changed. For the purpose of matching the downstream stator inlet airflow angle, the inverse modification of multiple S1 stream surfaces on the stator blade was carried out in this section. Then, the new geometry of certain stream surfaces was 3D stacked into a new stator vane. Afterwards, this is verified using the numerical simulation of the full 3D viscous solver, in order to redesign a compressor stage with better aerodynamic performance.

In this section, the pre-compression modified design rotor and original Stator 37, which constituted the stage and geometric parameters at 15%, 30%, 50% and 70% span, were selected along the spanwise direction, in order to respectively construct the S1 flow surface. The new geometry was obtained through inverse calculation, in order to achieve the design target of improving the aerodynamic performance of every stream surface.

For the stator-passage flow, large bend angles are often caused by the excessive flow separation at the trailing edge of the blade. Therefore, effectively reducing the bending angle of stator blades is the key to solving this problem.

The result refers to the comparison diagrams for the original, targeted, and calculated load distribution of every S1 stream surface of the stator, as shown in Fig. 16. As presented in the figure, the original load at the leading edge was larger, which led to a large angle of attack, and a local high-velocity zone appeared in front of the suction edge. Therefore, for the sake of achieving the redesign requirement of reducing the inlet angle of attack, and shrinking or eliminating the acceleration zone at the leading edge of the airfoil, this section adjusted the original load, in order to significantly diminish the target load at the leading edge, and make the targeted distribution smoother. Furthermore, the target load distribution initially rose in a small area, and this subsequently gradually decreased slowly, instead of presenting an overall downward trend for the original load distribution. These slows down the gradient of the load, and makes the flow become more reasonable.

Through the inverse calculation of the S1 flow surface, a comparison diagram for the blade geometry was made, as shown in Fig. 17. The black dotted line and green solid line represents the original blade profile and new profile, respectively. The appearance refers to the relatively obvious contrast between the two profiles, according to the figure. After the modification, the suction and pressure surface profiles significantly moved up. The closer this was to the tip where the surface was, the larger the displacement became. Therefore, due to the inverse design, the geometric bending angle of the blade profile significantly decreased, significantly reducing the turning angle when the air flows along the blade.

The distinctiveness of the blade geometry changes the flow field structure of the S1 flow surface. Figures 18-21 presents the comparison of flow field details, before and after the modification of the compressor stage. It can be noted from the figure that through the inverse design, when the air flows near the pressure surface, the low-velocity zone significantly decreased, and the flow was

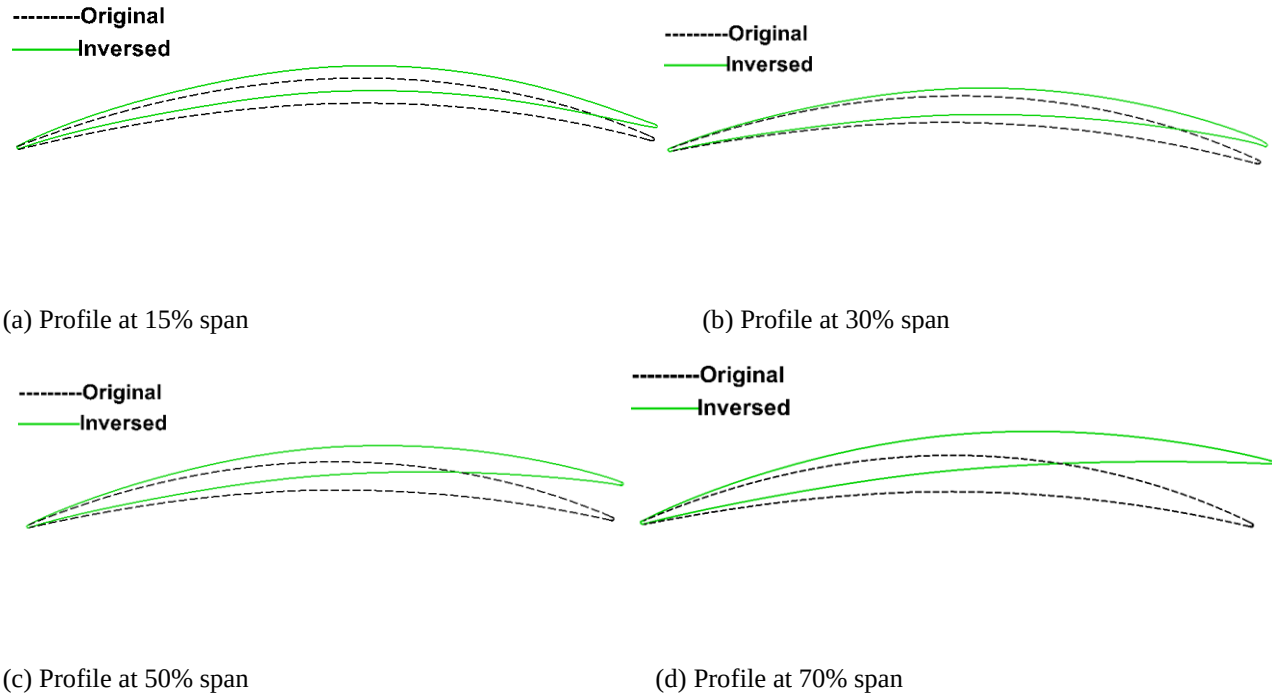

(a) Profile at 15% span (b) Profile at 30% span

(c) Profile at 50% span (d) Profile at 70% span

Fig. 17. Comparison for the original and inverse at the four spans.

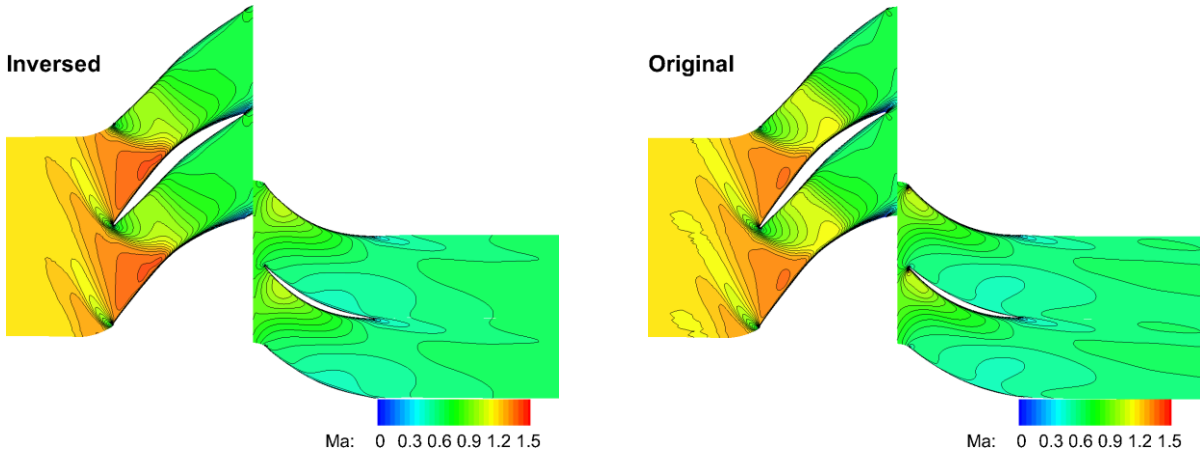

Fig. 18. Comparison of Ma contours between the original and redesigned S1 stream surface at 15% span of the stage.

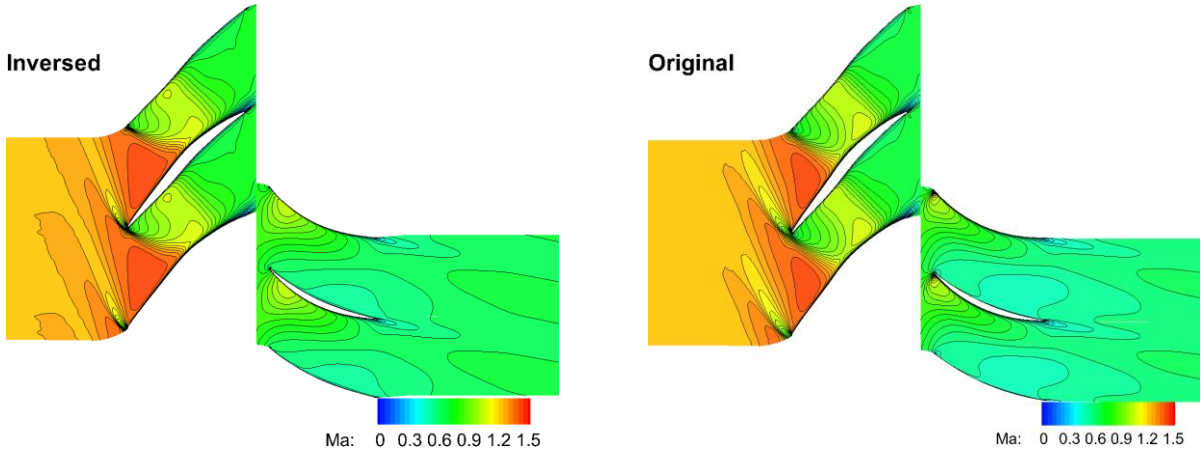

Fig. 19. Comparison of Ma contours between the original and redesigned S1 stream surface at 30% span of the stage.

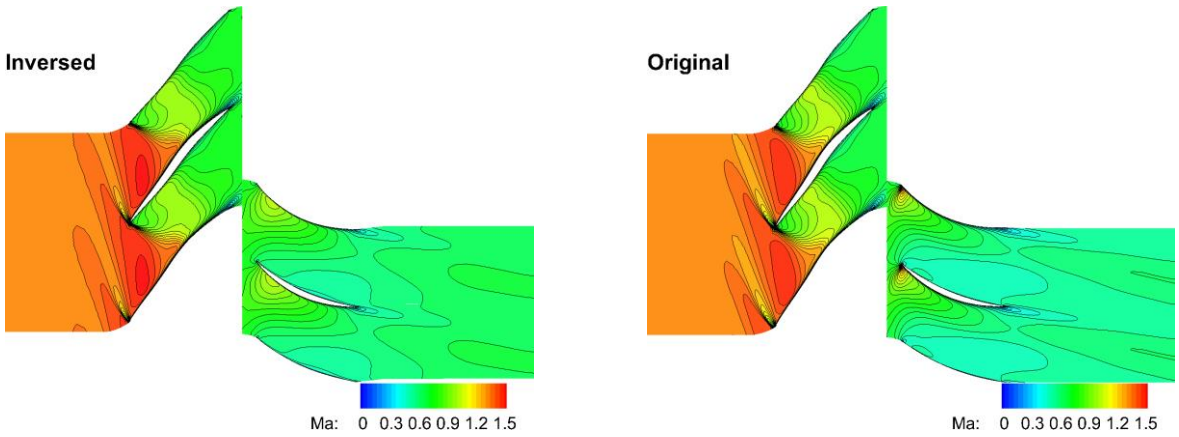

Fig. 20. Comparison of Ma contours between the original and redesigned S1 stream surface at 50% span of the stage.

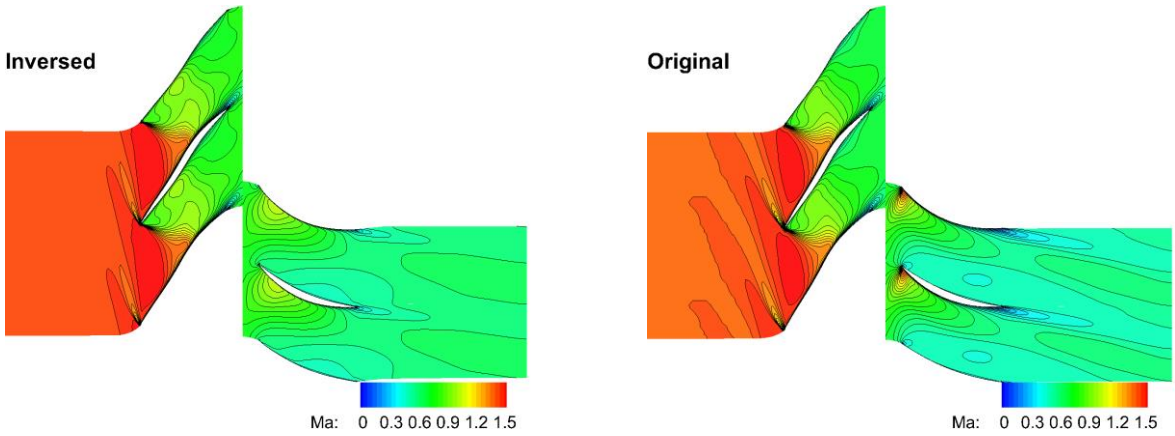

Fig. 21. Comparison of Ma contours between the original and redesigned S1 stream surface at 70% span of the stage.

Table 2 Aerodynamic parameter comparison at the design point for Stage 37

	Mass(Kg/s)	Adiabatic Efficiency	Pressure Ratio
Initial stage	20.987	0.846	2.098
New stage	21.024	0.850	2.143
Increasing percentage	0.18%	0.4%	4.5%

more reasonable. On the other hand, based on the leading edge of the suction surface, the acceleration area was basically eliminated. Therefore, the flow situation in the stator along each S1 flow surface significantly improved after the modification, basically reaching the desired effect proposed at the beginning of this section.

After the modification design of the corresponding S1 stream surface was accomplished for the stator, it was correspondingly indispensable to verify the aerodynamic performance of the new stage, which comprised of the pre-compression rotor and stator stacking of blade profiles calculated above. Similarly, the flow field of the modified stage was calculated by the full three-dimensional viscous method. Simultaneously, the comparison of the pressure ratio and adiabatic efficiency characteristic curve between the two stages became significant for obtaining a compressor stage with better overall performance. This further verified the feasibility and effectiveness of the inverse method employed in the present study.

In order to better present the comparison of the performance of the new stage with that of the original stage, the aerodynamic parameters at the near-peak-efficiency point were listed in Table 2. Obviously, the mass flow, pressure ratio, and adiabatic efficiency of the new stage improved.

The characteristic curves for pressure ratio and adiabatic efficiency at a stable operating range is presented in Fig. 22.

As shown in the figure, the efficiency and pressure ratio of the modified stage was higher, when compared to that of the original stage, in the whole working range. In general, the aerodynamic performance of the new stage was better, when compared to that of the original stage, basically meeting the expected design requirements, and realizing the purpose of designing a better compressor stage.

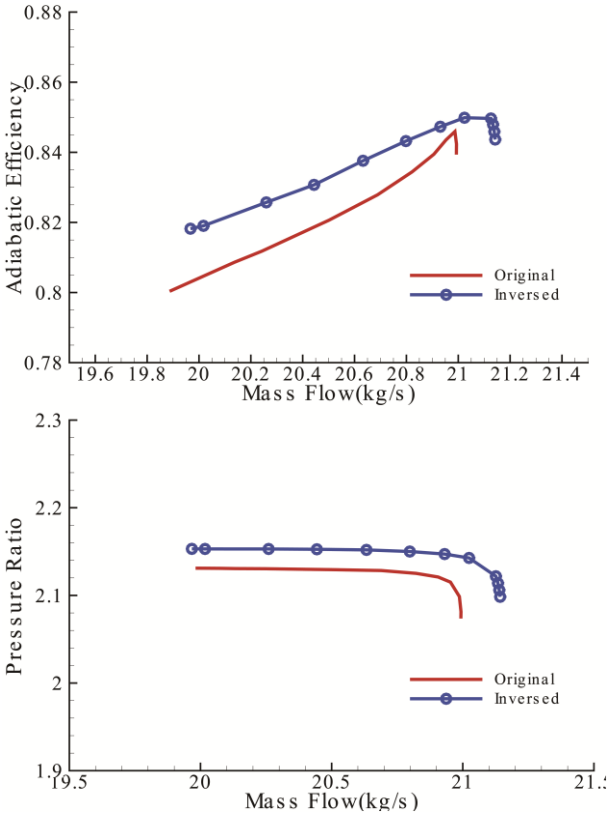

Fig. 22 Comparison of the adiabatic efficiency and pressure ratio between the original and redesigned Stage 37.

5. CONCLUSIONS

Based on the research on CFD, which has become increasingly mature, the load-camber method of the inverse design theory, which unites a quasi-three-dimensional solver, was established using the no-slip boundary condition. The reliability and effectiveness were validated by conducting two inverse cases, namely, Rotor 37 and Stage 37. The aerodynamic performance of these two cases was compared between the original and inverse one. As a result, this can be concluded, as follows:

(1) The inverse method of the S1 stream surface modifies the load distribution of the selected design surfaces along the span, according to a reasonable flow characteristic, while the load distribution calculated along the axial direction was coincident with the target distribution. The design intention of promoting the S1 stream surface aerodynamic performance was achieved.

(2) A rotor blade and a single-stage compressor were stacked after obtaining the new geometry of the designed S1 stream surfaces. Compared to the original one, the flow mass, pressure ratio and adiabatic efficiency of the redesigned rotor and stage improved at the on-design point, the stable working range became wider, and the overall aerodynamic performance of the new one exhibited a better effect. It was suggested that the inverse method well-meets the initial design requirements, and it was validated that the method has preferable effectiveness and reliability.

(3) The inverse design method of the S1 stream surface only studies some of the design stream surfaces along the blade spanwise. This shortens the calculation time, and improves the computational efficiency of the inverse method, when compared to the three-dimensional method. The present method broadens the application scope of the inverse method, and provides a new design concept for the development of the inverse method.

CONFLICT OF INTEREST

The authors declared no potential competing financial interests with respect to the research, authorship, and/or publication of this article.

AUTHORS CONTRIBUTION

H, Lou: Conceptualization; Methodology; Software; Validation; Formal analysis; Data Curation; Writing - Original Draft & Editing

H, Wu: Supervision; Writing – Review; Funding acquisition

Q, Tang: Writing – Review

L, Deng: Writing – Review

REFERENCES

Ahmadi, M., & Ghaly, W. S. (1998). Aerodynamic inverse design of turbomachinery cascades using a finite volume method on unstructured meshes. *Inverse Problems in Engineering*, 6, 281–298. https://doi.org/10.1080/174159798088027680

Baldwin, B. S. (1978, January). *Thin-layer approximation and algebraic model for separated turbulent flows*. American Institute of Aeronautics and Astronautics, Aerospace Sciences Meeting, Huntsville, Ala.

Blazek, J. (2015). *Computational Fluid Dynamics: Principles and Applications*. Butterworth-Heinemann.

Chu, W., Liu, Q., & Hu, C. (2009). *Principles of Aviation Vane Machines.* Northwest University of Technology Press.

Dang, T. (1995, January). *Inverse method for turbomachine blades using shock-capturing techniques*. 31st Joint Propulsion Conference and Exhibit.

Dang, T. Q. (1993). A fully three-dimensional inverse method for turbomachinery blading in transonic flows. *Journal of Turbomachinery* 115, 354-361. https://doi.org/10.1115/1.2929241

Hawthorne, W. R., Wang, C., Tan, C. S., & McCune, J. E. (1984). Theory of blade design for large deflections: Part I—Two-dimensional cascade. *Journal of Engineering for Gas Turbines & Power*, 106, 346–353. https://doi.org/10.1115/1.3239571

Hield, P. (2008, January). *Semi-inverse design applied to an eight-stage transonic axial flow compressor*. Turbo Expo: Power for Land, Sea, and Air.

Hu, J. (2014). *Principles of aviation vane machines*. National Defense Industry Press.

Jameson, A., Schmidt, W., & Turkel, E. (1981, June). *Numerical solution of the Euler equations by finite volume methods using Runge Kutta time stepping schemes*. 14th fluid and Plasma Dynamics Conference, Palo Alto, CA.

Lighthill, M. J. (1945). A new method of two-dimensional aerodynamic design. *Aeronautical Research Council R and M* 2112. https://citeseerx.ist.psu.edu/viewdoc/download;jsessionid=7C78BA426572BDA97B4D0E6EE7F17043?doi=10.1.1.226.6595&rep=rep1&type=pdf

Liu, Z. (2017). *Research of full three-dimensional viscous inverse design method for multi-stage axial compressor*. [PhD. thesis, Northwestern Polytechnical University]. Shaanxi, China.

Liu, Z., Wu, H., & Tang, X. (2015). Application of improved inverse method boundary condition in turbomachiny. *Journal of Engineering Thermophysics*, 36, 2132–2136. https://kns.cnki.net/kcms2/article/abstract?v=3uoqIhG8C44YLTlOAiTRKibYlV5Vjs7ir5D84hng_y4D11vwp0rrtYebZZdUY3FI3MkboggYCoQtc_s0u_IXGkFPdma8AsYm&uniplatform=NZKPT

Medd, A. J., Dang, T. Q., & Larosiliere, L. M. (2003, January). *3D inverse design loading strategy for transonic axial compressor blading*. Turbo Expo: Power for Land, Sea, and Air.

Suder, K. L. (1996). *Experimental Investigation of the Flow Field in A Transonic, Axial Flow Compressor with Respect to the Development of Blockage and Loss*. Case Western Reserve University.

Tan, C. S., Hawthorne, W. R., McCune, J. E., & Wang, C. (1984). Theory of blade design for large deflections: Part II—annular cascades.

Tiow, W. T., & Zangeneh, M. (2000, May). *A three-dimensional viscous transonic inverse design method*. Turbo Expo: Power for Land, Sea, and Air.

van Rooij, M., and Medd, A. (2012, June). Reformulation of a three-dimensional inverse design method for application in a high-fidelity CFD environment. In *Turbo Expo: Power for Land, Sea, and Air* (Vol. 44748, pp. 2395-2403). https://doi.org/10.1115/GT2012-69891

Wu, C. H. (1952). *A general theory of three-dimensional flow in subsonic and supersonic turbomachines of axial-, radial, and mixed-flow types*. National Aeronautics and Space Administration Washington DC.

Yang, C., Wu, H., and Liang, Y. (2019). A novel three-dimensional inverse method for axial compressor blade surface design. *Arabian Journal for Science and Engineering*, 44(12), 10169-10179. https://doi.org/10.1007/s13369-019-04083-3

Yang, J., Liu, Y., Wang, X., & Wu, H. (2016, June). *3D viscous inverse design of turbomachinery using one-equation turbulence model*. Turbo Expo: Power for Land, Sea, and Air.

Yang, J., Liu, Y., Wang, X., & Wu, H. (2017). An improved steady inverse method for turbomachinery aerodynamic design. *Inverse Problems in Science and Engineering*, 25(5), 633-651. https://doi.org/10.1080/17415977.2016.1178259

Yang, J., Liu, Z., Shao, F., & Wu, H. (2015). Transpiration boundary condition based on inverse method for turbomachinery aerodynamic design: on the solution existence and uniqueness. *Journal of Propulsion Technology*, (4), 579–586. https://doi.org/10.13675/j.cnki.tjjs.2015.04.014

Zangeneh, M., Goto, A., & Harada, H. (1998). On the design criteria for suppression of secondary flows in centrifugal and mixed flow impellers. *Journal of Turbomachinery*, 120, 723–735. https://doi.org/10.1115/1.2841783

Zangeneh, M., Goto, A., & Harada, H. (1999). On the role of three-dimensional inverse design methods in turbomachinery shape optimization. *Proceedings of the Institution of Mechanical Engineers, Part C: Journal of Mechanical Engineering Science*, 213(1), 27-42. https://doi.org/10.1243/0954406991522167